

Evaluation of adrenal tumors by magnetic resonance imaging with histological correlation*

Avaliação por ressonância magnética dos tumores de adrenal com correlação histológica

Daniel Lahan Martins¹, Ronaldo Hueb Baroni², Roberto Blasbalg², Públio Cesar Cavalcanti Viana³, Regis Otaviano Franca Bezerra³, Francisco Donato Jr.³, Romulo Loss Mattedi⁴, Antonio Marmo Lucon⁵, Claudia da Costa Leite⁶, Giovanni Guido Cerri⁷

Abstract Magnetic resonance imaging is an important tool for the detection and characterization of adrenal tumors. The knowledge about the different presentations of primary and secondary adrenal tumors at magnetic resonance imaging and their correlation with histological data are essential for the establishment of a correct diagnosis. The present study reviews magnetic resonance imaging aspects which may narrow the differential diagnosis of adrenal tumors, emphasizing the histological correlation of the most frequent ones.

Keywords: Magnetic resonance imaging; Adrenal glands; Retroperitoneal neoplasms; Urogenital neoplasms; Imaging diagnosis.

Resumo A ressonância magnética é ferramenta importante para a detecção e caracterização dos tumores adrenais. O conhecimento das diferentes apresentações dos tumores primários e secundários à ressonância magnética e sua correlação com dados da histologia são essenciais para o correto raciocínio diagnóstico. Este artigo revisa os aspectos que podem estreitar o diagnóstico diferencial dos tumores adrenais, dando ênfase à correlação histológica daqueles mais comuns.

Unitermos: Imagem por ressonância magnética; Glândulas supra-renais; Neoplasias retroperitoneais; Neoplasias urogenitais; Diagnóstico por imagem.

Martins DL, Baroni RH, Blasbalg R, Viana PCC, Bezerra ROF, Donato Jr F, Mattedi RL, Lucon AM, Leite CC, Cerri GG. Avaliação por ressonância magnética dos tumores de adrenal com correlação histológica. *Radiol Bras.* 2008;41(1):55–62.

INTRODUCTION

The name “adrenal gland” comes from its localization adjacent to the kidneys (*ad-renal*). A normal adrenal gland weights 5 g, presents a typical inverted Y-, V-, or T-

shape, and consists of cortex (cortisol, aldosterone and androgens secretion) and medulla (epinephrine and norepinephrine secretion). The normal adrenal body measures up to 10–12 mm, and its limbs not more than 5–6 mm. The right adrenal gland lies immediately posterior to the inferior vena cava and superiorly to the right kidney. At left, the gland lies anteromedial to the upper pole of the left kidney. They are retroperitoneal structures contained within the Gerota’s fascia. The renal fascia involves the adrenal glands, but a transverse fibrous lamella joins their ventral layer with the dorsal layer of the renal fascia, allowing their separation from the kidney during nephrectomy. There is fat involving the adrenal glands^(1,2).

Adrenal glands can be easily visualized on abdominal magnetic resonance imaging (MRI). Typically they appear isointense or

hypointense to the liver. MRI is frequently utilized to evaluate adrenal lesions diagnosed by means of other methods such as CT, in cases where they are inconclusive. Also, adrenal lesions (the so called incidentalomas) are frequently incidentally found at MRI performed for investigating other abnormalities.

MRI offers an exceptional contrast resolution, achieving a good spatial resolution in the evaluation of adrenal glands, including for detection of lesions as small as 0.5–1.0 cm. The MRI protocol should include high-resolution, multiplanar, T1-weighted images (5 mm-thick at maximum) for anatomical details, and T2-weighted images. Fat suppression is utilized to avoid images degradation by chemical shift artifacts caused by the fat involving the adrenal gland^(2,3).

In-phase and out-of-phase gradient-echo (GRE) sequences are essential for allowing the detection of microscopic intratumoral fat, increasing the specificity of the method and avoiding unnecessary interventions⁽⁴⁾.

* Study developed at Instituto de Radiologia do Hospital das Clínicas da Faculdade de Medicina da Universidade de São Paulo (InRad/HC-FMUSP), São Paulo, SP, Brazil.

1. Specialist in Radiology and Imaging Diagnosis, MD, Researcher at Instituto de Radiologia do Hospital das Clínicas da Faculdade de Medicina da Universidade de São Paulo (InRad/HC-FMUSP), São Paulo, SP, Brazil.

2. PhDs, Physician Assistants at Instituto de Radiologia do Hospital das Clínicas da Faculdade de Medicina da Universidade de São Paulo (InRad/HC-FMUSP), São Paulo, SP, Brazil.

3. Specialists in Radiology and Imaging Diagnosis, Instituto de Radiologia do Hospital das Clínicas da Faculdade de Medicina da Universidade de São Paulo (InRad/HC-FMUSP), São Paulo, SP, Brazil.

4. MD, Pathologist, Department of Pathology, Instituto de Radiologia do Hospital das Clínicas da Faculdade de Medicina da Universidade de São Paulo (InRad/HC-FMUSP), São Paulo, SP, Brazil.

5. Professor, Division of Clinical Urology, Hospital das Clínicas da Faculdade de Medicina da Universidade de São Paulo (HC-FMUSP), São Paulo, SP, Brazil.

6. Private Docent, Head for the Unit of Magnetic Resonance Imaging, Instituto de Radiologia do Hospital das Clínicas da Faculdade de Medicina da Universidade de São Paulo (InRad/HC-FMUSP), São Paulo, SP, Brazil.

7. Full Professor, Division of Radiology, Hospital das Clínicas da Faculdade de Medicina da Universidade de São Paulo (InRad/HC-FMUSP), São Paulo, SP, Brazil.

Mailing address: Dr. Daniel Lahan Martins, Rua Alves Guimarães, 518, ap. 51, Pinheiros. São Paulo, SP, Brasil, 05410-000. E-mail: daniel_lahan@hotmail.com

Received July 17, 2007. Accepted after revision August 24, 2007.

Some adrenal tumors are hyperfunctional (excessive production of cortisol, aldosterone and/or androgens). Cushing's syndrome (excessive production of cortisol) is typically secondary to hypophyseal adenomas, unless in cases resulting from adrenal tumors, where, most frequently, benign adenomas are the cause of the disease. Hyperaldosterism resulting from adrenal adenoma (80% of cases) is known as Conn's syndrome⁽⁵⁾.

ADRENOCORTICAL TUMORS

Adenoma

The adenomas incidence in the general population is estimated in 2% to 8%⁽⁶⁾. Most frequently, adrenal adenomas are nonfunctional tumors, however, in cases of functional tumors, specific clinical symptoms represent a warning of the presence of an adrenal tumor. Nonfunctional adenomas usually constitute incidental findings^(3,7).

The majority of adenomas are slightly hypointense or isointense to the liver on T1-weighted images, and slightly hyperintense or isointense on T2-weighted images.

The utilization of chemical-shift techniques (in-phase- or out-of-phase GRE) allows the characterization of adenomas containing microscopic fat and water protons in a same voxel (Figure 1). On out-of-phase images, the protons signal is null and results in signal loss as compared with in-phase-images^(3,4,7,8). Some authors quantify this signal loss, considering a decrease of > 20% as compatible with the diagnosis of adenoma⁽⁹⁾.

Although highly suggestive of adenoma, these findings are non-specific. Other adrenal lesions may include microscopic fat and, consequently, signal loss in out-of-phase sequences. This occurs in some cases of adrenal carcinoma, metastatic renal cells carcinoma, hepatocellular carcinoma metastasis, etc.^(3,7,9). So, other parameters than signal loss should be taken into consideration in the diagnosis of adenoma: the lesion must be homogeneous, < 5 cm in size and present regular margins^(3,7,9).

Carcinoma

Adrenocortical carcinoma is a rare neoplasm most frequently occurring between

the fourth and fifth decades of life and equally prevalent for both men and women. Typically, they present as large lesions (> 5,0 cm) at the moment of the diagnosis and may include necrosis, bleeding and, frequently, calcification⁽⁶⁾.

About 25% to 50% of adrenal carcinomas are rated as functional, and most of times cause Cushing's syndrome^(6,10). Generally, primary adrenocortical carcinomas are unilateral. MRI has been considered as method superior to CT in the staging of this disease, allowing a better evaluation in cases of adjacent organs invasion⁽⁷⁾.

Signal intensity in adrenal carcinomas is variable, usually heterogeneous on T1- and T2-weighted sequences (Figure 2). Usually, after contrast injection, the lesion is heterogeneously enhanced.

Considering that this neoplasm originates in the adrenal cortex, microscopic fat may be present, similarly to adenomas, possibly resulting in signal loss on out-of-phase GRE sequences⁽¹¹⁾. Most frequently, however, the differential diagnosis with adenoma is not difficult. In carcinomas, only part of the lesion loses signal intensity (het-

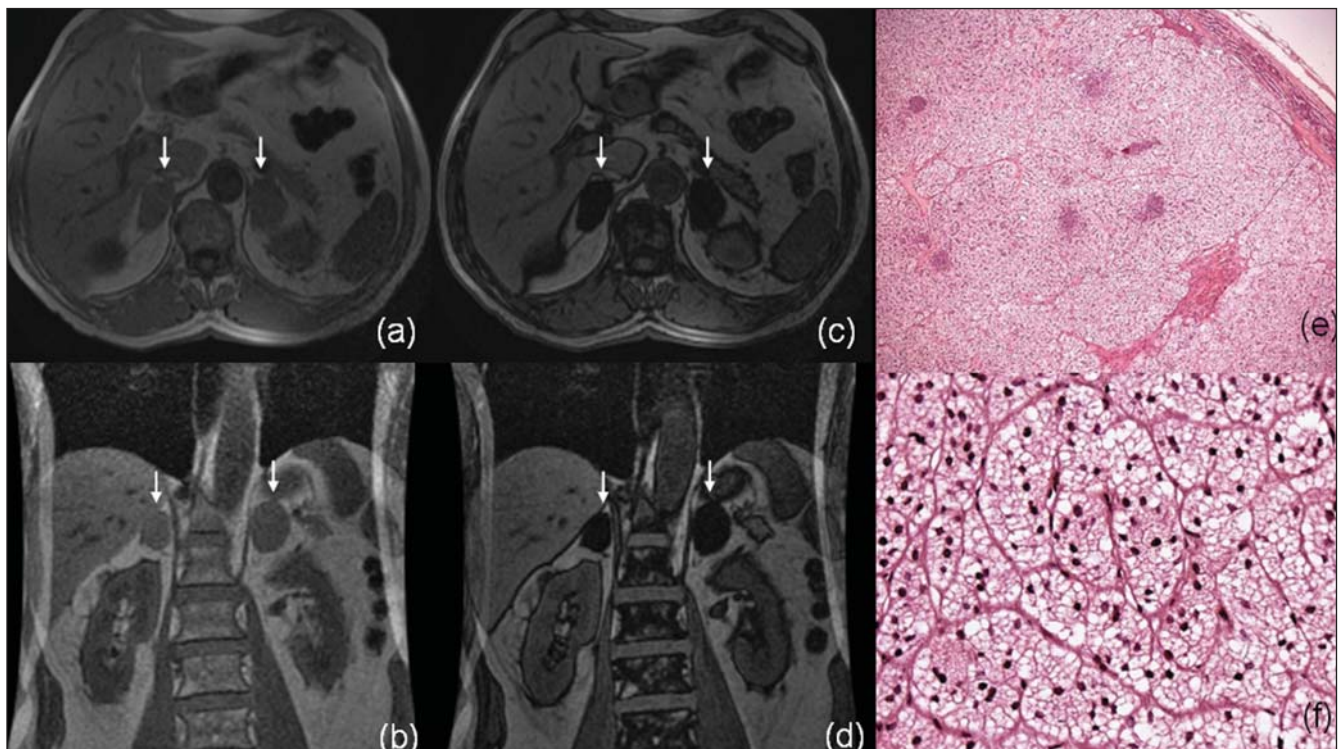


Figure 1. MRI axial T1-weighted phase-GRE (a) and coronal (b) sequences demonstrate bilateral adrenal lesion (arrows). Axial (c) and coronal (d) out-of-phase sequences demonstrate adrenal lesions signal loss, allowing the diagnosis of microscopic lipid-rich adenoma. e: Hematoxylin-eosin (HE), 50× – delimited cortical lesion demonstrating interface with the remaining gland with atrophic aspect (right upper corner). f: HE, 400× – neoplasm constituted by cells without atypias, with low nuclear grade, wide and clear cytoplasm in trabecular and nest dispositions.

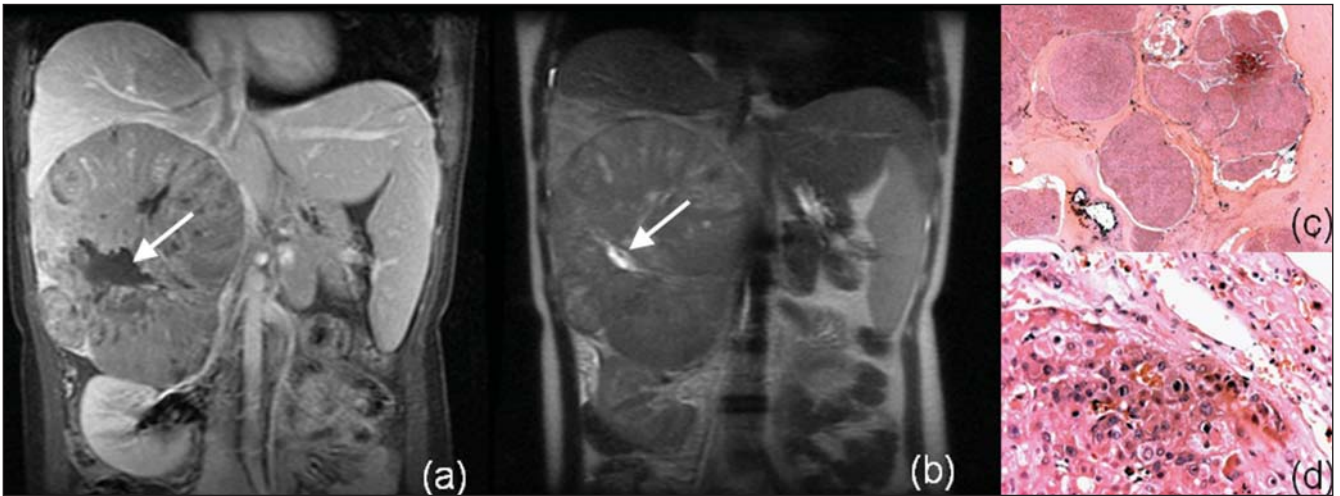


Figure 2. Adrenal cortical carcinoma. MRI contrast-enhanced coronal T1-weighted GRE (a) and coronal T2-weighted SS-FSE (b) sequences demonstrate a large expansive lesion involving the right adrenal gland. The lesion shows heterogeneous pattern of impregnation by the contrast agent and areas of necrosis (hypersignal on T2-weighted sequences)(arrows). Neoplasm with multinodular architecture, with eosinophil cells and calcification foci – HE, 12.5× (c); Images of mitosis in neoplastic cells – HE, 400× (d).

erogeneously), besides the fact that the tumor is larger in size and presents with heterogeneous signal^(3,7,9).

Myelolipoma

Generally, myelolipomas are benign, unilateral, non-functioning lesions composed of fat and bone marrow in varying proportions. Calcifications may be found in 20% of cases⁽¹²⁾. Most frequently, these

lesions are asymptomatic or present with pain (in cases of hemorrhage or compression of adjacent structures)⁽¹³⁾.

The diagnosis of myelolipoma consists in demonstrating macroscopic fat in the adrenal lesion. At MRI, this type of fat presents hyperintense signal on T1-weighted images. This finding by itself is non-specific, considering that it also can be found in hemorrhagic lesions. A fat suppression

sequence should be performed for comparison, observing a loss of signal intensity of the macroscopic fat, which is compatible with the diagnosis of myelolipoma (Figure 3). Myelolipomas, also, may be diagnosed on chemical-shift sequences, the “India ink” artifact being identified in the interface between fat and soft tissues in the lesion. Myelolipomas with larger amounts of adipose tissue compressing the adjacent

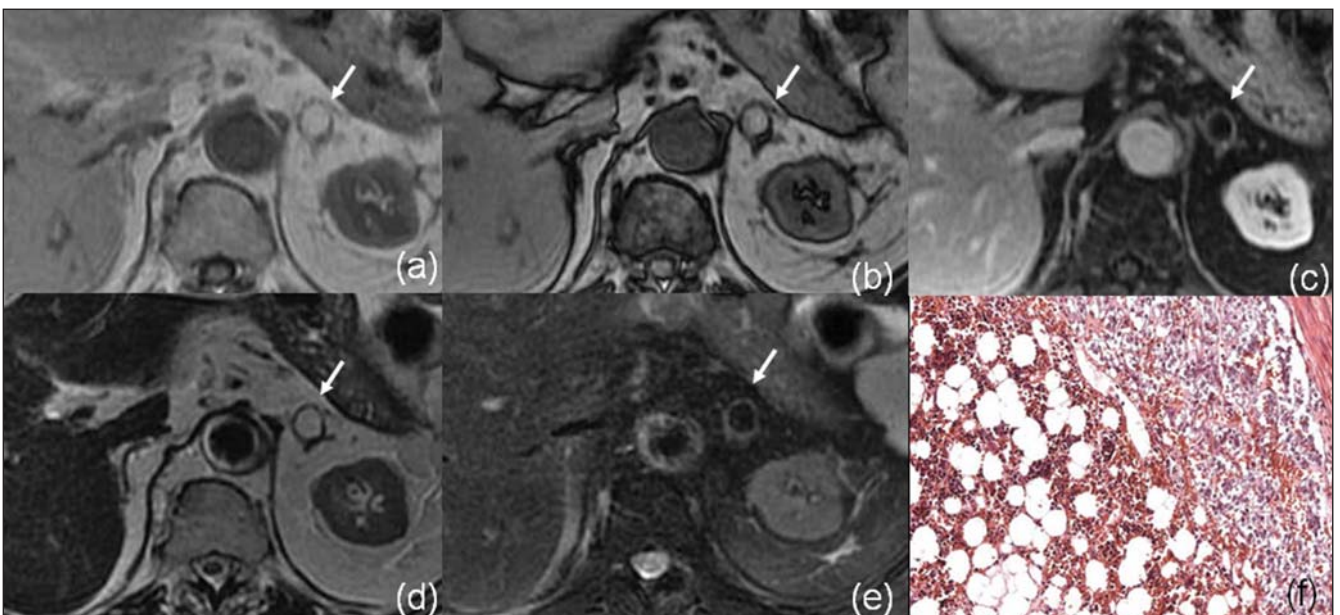


Figure 3. MRI axial T1-weighted phase- (a) and out-of-phase GRE (b), contrast-enhanced, axial T1-weighted (c), axial T2-weighted (d) and axial, T2-weighted sequence with fat-suppression (e): arrows demonstrate typical features of myelolipoma in the left adrenal gland, with macroscopic fat component signal loss with fat-saturation (c,e). HE, 200× (f) demonstrating hematopoietic tissue (erythrocytes, granulocytes and megakaryocytes) associated with the adrenal tissue.

organs may be confused with a low grade retroperitoneal liposarcoma or even an exophytic renal angiomyolipoma. However, usually on multiplanar images, the origin of the lesion can be demonstrated⁽³⁾.

ADRENAL MEDULLARY TUMORS

Pheochromocytoma

Pheochromocytomas are rare tumors arising from pheochromocytes, the predominant cells in the adrenal medulla⁽¹⁴⁾. These tumors are most frequently found between the fourth and sixth decades of life. Approximately 10% are bilateral, 10% are malignant, 10% occur in children, and 10% are extra-adrenal⁽¹⁵⁾.

More than 90% of pheochromocytomas arise in the adrenal gland, and 98% are intraabdominal. Extra-adrenal pheochromocytomas develop in paraganglion chromaffin cells of the sympathetic nervous system, may occur at any site from the base of the skull to the bladder, and are called paragangliomas⁽¹⁶⁾.

Although the majority of patients with pheochromocytoma present with manifestations resulting from excessive secretion of catecholamine, approximately 10% of these patients are asymptomatic, the tumor being incidentally detected by means of imaging studies performed by other reasons⁽¹⁷⁾.

Pheochromocytomas and paragangliomas present different appearances at different imaging methods. Variable degrees of pathological degeneration may occur, and, consequently, a wide spectrum of imaging characteristics may be found⁽¹⁸⁾.

Its main manifestation at MRI is an expansive lesion with low signal intensity on T1-weighted sequences, and high signal intensity on T2-weighted sequences (even higher on T2-weighted sequences with fat saturation because of the decrease in signal of adjacent fat tissue). Generally, these tumors are intensely enhanced after contrast agent injection⁽¹⁸⁾ (Figure 4). However, its aspect may vary at MRI, including the possibility of finding of pheochromocytomas with low signal intensity on T2-weighted sequences^(18,19).

There is a considerable overlapping among MRI findings of pheochromocytomas and other adrenal tumors. Approximately 35% of pheochromocytomas are erroneously classified as malignant lesions or adenomas, particularly in cases of atypical images on T2-weighted sequences⁽¹⁹⁾. The diagnosis of pheochromocytomas cannot be excluded only on the basis on the absence of hyperintense signal on T2-weighted sequences. Similarly, other tumors (including some metastases) may be erroneously classified as pheochromocytomas only on the basis of the finding of hyperintense signal on T2-weighted sequences.

Neuroblastoma

Although neuroblastomas are the third most frequent malignant tumors in children, they are much less frequent in adults. This tumor occurs at any site along the parasympathetic nervous system. The most disseminated form of the disease is more frequent in adults than in children. The lack of specificity of imaging findings, and fre-

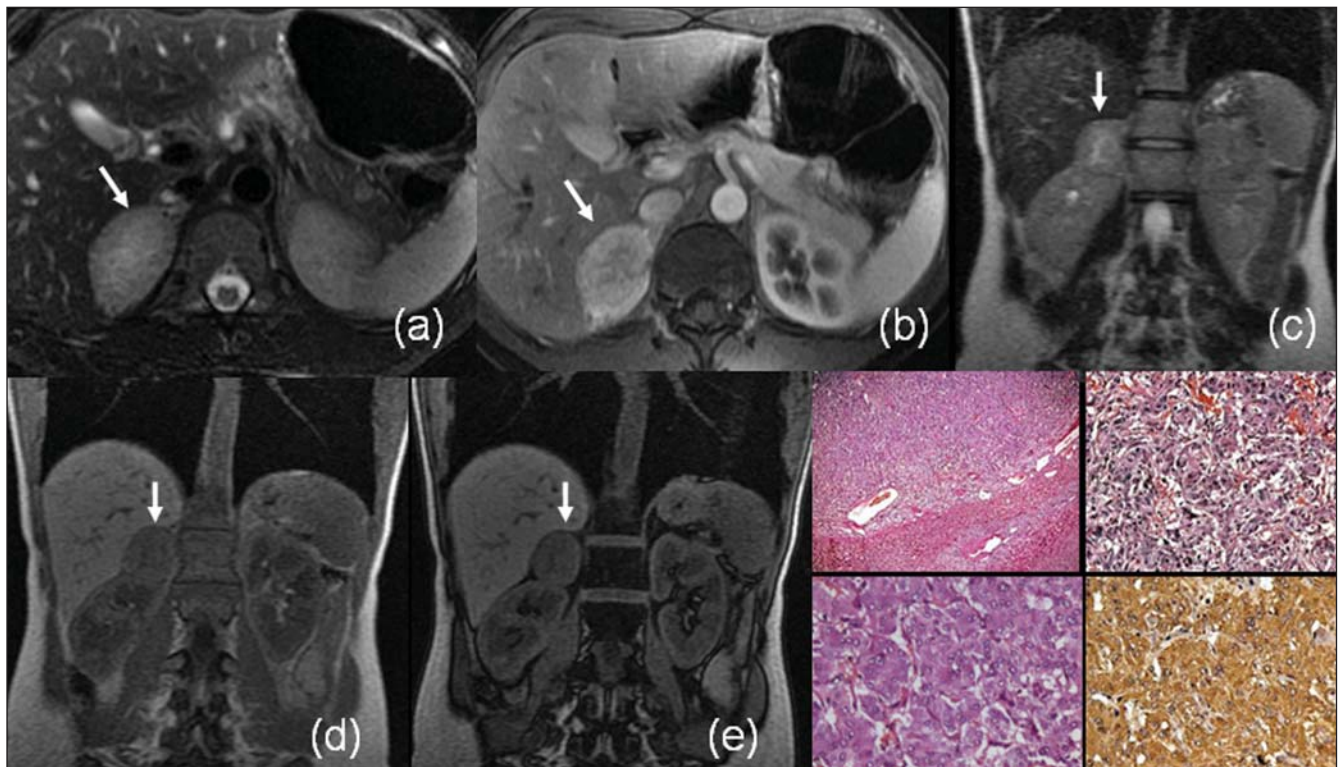


Figure 4. MRI axial, FSE T2-weighted (a), axial, contrast-enhanced GRE, T1-weighted (b), coronal SS-FSE T2-weighted (c), coronal in-phase-GRE T1-weighted (d) and out-of-phase GRE T1-weighted sequences (e) demonstrate a pheochromocytoma (arrows). Typical absence of signal loss on out-of-phase sequences, remarkable hyperintense signal on T2-weighted sequences and increased contrast uptake. Histological study (left lower corner) shows adrenal medullary neoplasm with basophil cytoplasm, chromaffin cells and classic Zellballen pattern. Immunohistochemical staining for chromogranin A antibody.

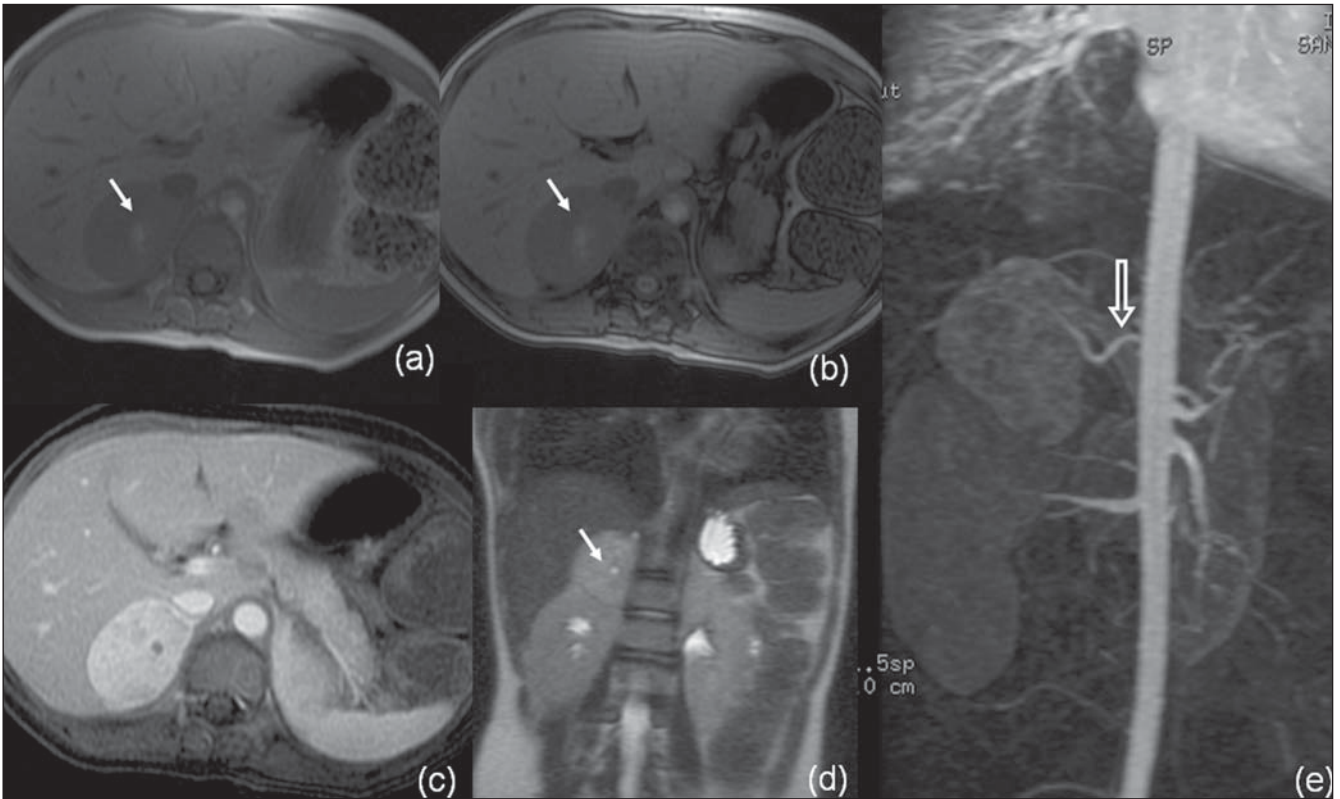


Figure 5. MRI axial, in-phase (a) and out-of-phase (b) GRE T1-weighted, coronal SS-FSE T2-weighted (d) sequences of right adrenal neuroblastoma. The tumor is predominantly hypointense on T1-weighted sequences and presents a central hemorrhagic area with hyperintense signal (arrows on a, b and d). Contrast uptake (c). MRI angiography (e) demonstrates right adrenal irrigation (open arrow) of relevance for surgical planning.

quent disseminated involvement suggest lymphoma and metastasis as the main differential diagnosis⁽¹⁶⁾.

Neuroblastomas usually present heterogeneous low signal intensity on T1-weighted sequences, high signal intensity on T2-weighted sequences and paramagnetic contrast uptake. Calcifications occur in 80–90% of cases, but their detection is difficult at MRI. Areas of intratumoral hemorrhage appear with a typical hyperintense signal on T1-weighted sequences, and cystic alterations present high signal intensity on T2-weighted sequences (Figure 5). MRI has been considered as more sensitive than CT in the diagnosis of these tumors, thanks to its contrast high-resolution⁽²⁰⁾.

LYMPHOMA

Primary adrenal lymphoma is rarely found^(21,22), differently from the secondary involvement where other retroperitoneal site is involved. This is more usual in cases of non-Hodgkin lymphomas than in cases

of Hodgkin's disease⁽²³⁾. Generally, the involvement is bilateral.

Adrenal lymphomas manifestations may range from small lesions to a more diffuse involvement where the adrenal glands maintain their adreniform shape. Also, an extensive involvement may occur, making the identification of the adrenal gland impossible⁽¹⁶⁾.

At MRI, lymphomas present a lower signal intensity than the liver on T1-

weighted sequences, and is typically hyperintense and heterogeneous on T2-weighted images (Figure 6). A discreet contrast uptake is observed^(2,16).

METASTASES

Metastases are the most frequent malignant tumors occurring in the adrenals, and are found in up to 27% of autopsies in patients with malignant epithelial tumors.

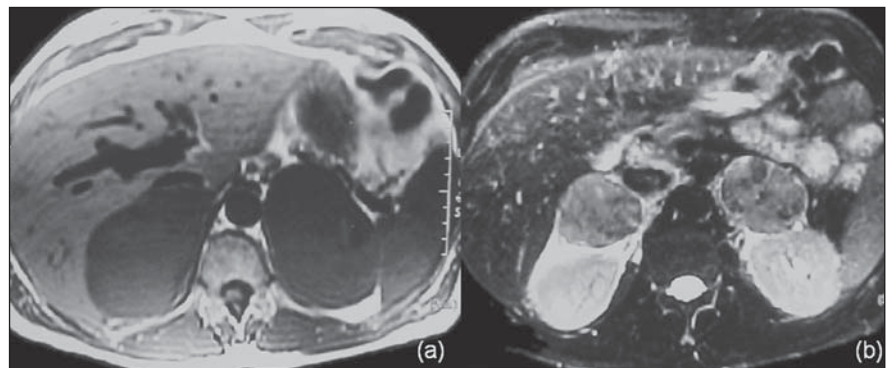


Figure 6. MRI axial T1-weighted (a) and T2-weighted (b) images of bilateral adrenal lesion in an HIV+ patients. Percutaneous biopsy was performed with diagnosis of non-Hodgkin lymphoma.

Lungs colon, breast and pancreas are the most common primary sites to metastasize to the adrenals⁽²⁾.

Some criteria are suggestive of malignant adrenal lesions at MRI, like diameter > 5 cm, irregular margins, invasion of adjacent structures and enlargement observed along the follow. Additionally, adrenal metastases use to appear hypo- or isointense to the liver on T1-weighted sequences, and with high intensity signal on T2-weighted images⁽⁵⁾ (Figures 7 e 8).

Metastases from renal cell carcinomas, hepatocellular carcinomas and liposarcomas may include microscopic fat and, consequently, may be seen with signal intensity loss on out-of-phase sequences (Figure 9). Generally, metastases present a persistent uptake after contrast injection, but with a pattern that may range accordingly to the primary tumor⁽⁷⁾.

PSEUDOTUMORAL CONDITIONS

Adrenal hyperplasia

Adrenal cortical hyperplasia may be primary or secondary (hypophyseal/hypothalamic lesions, or lesions resulting from ectopic of adrenocorticotrophic hormone [ACTH]). It is most frequently found in Conn's syndrome or adrenogenital syndrome. In patients with hyperaldosterism, the differentiation between hyperplasia and adenoma defines if a clinical or surgical conduct should be adopted⁽²⁴⁾. In adrenal hyperplasia, the glands present bilaterally thickened, although maintaining their adreniform shape, and generally with regular margins⁽²⁵⁾. Less frequently, hyperplasia may manifest as a nodular thickening, or even not changing the normal adrenals shape (Figure 10). It is important to remember that bilateral adrenal nodules are non-specific for hyperplasia⁽²⁾.

Adrenal cysts, pseudocysts and hemorrhages

Adrenal cysts and pseudocysts are rare and generally are incidentally diagnosed by means of imaging methods. Patients with this type of lesion are asymptomatic, unless the lesion grows sufficiently to result in a mass effect in adjacent organs. Adrenal cysts have been divided into four main categories: 1) endothelial (angiomatous or

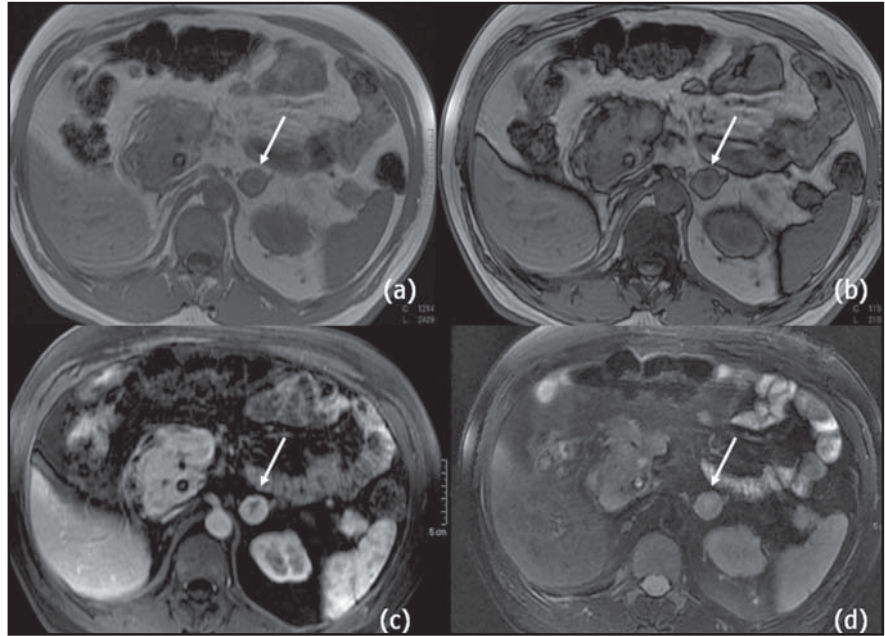


Figure 7. MRI axial in-phase (a) out-of-phase (b) GRE T1-weighted sequences, contrast enhanced T1-weighted (c) and T2-weighted with fat saturation sequences (d) demonstrate heterogeneous contrast agent uptake in metastasis of renal cell carcinoma to left adrenal gland (arrows).

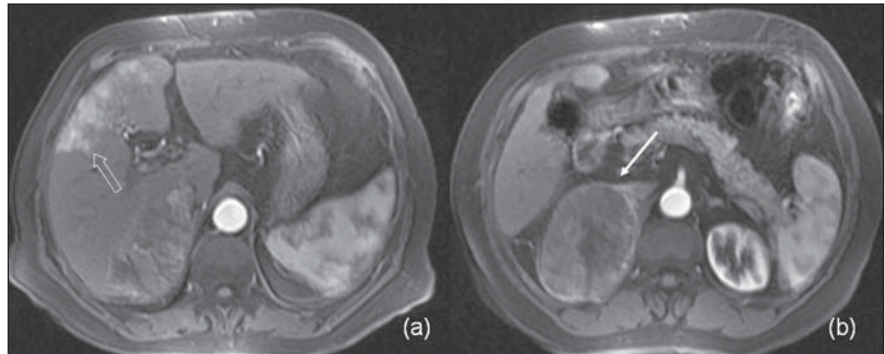


Figure 8. Contrast-enhanced MRI axial T1-weighted images demonstrate heterogeneous contrast agent uptake in right adrenal metastasis (arrow on b) of hepatocellular carcinoma (open arrow on a).

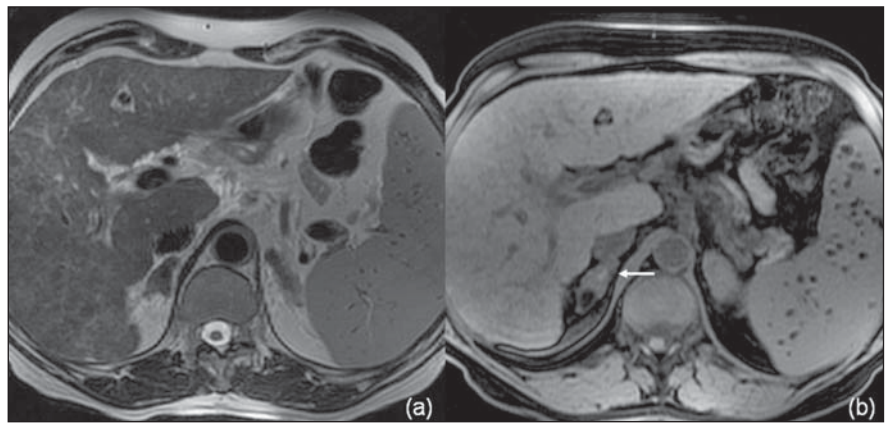


Figure 9. MRI axial T2-weighted (a) and T1-weighted (b) sequences of a patient with known melanoma and adrenal lesions. Arrow on b demonstrates a high intensity signal component compatible with melanin (metastasis).

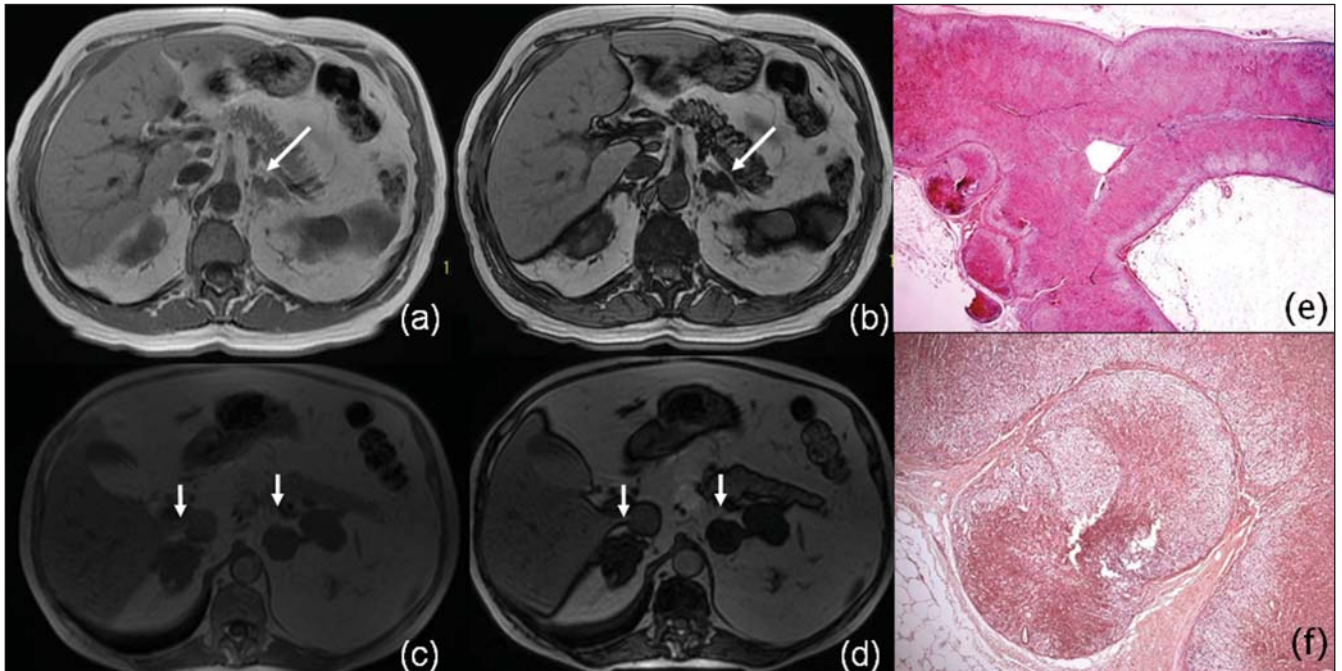


Figure 10. MRI axial in-phase (a) and out-of-phase (b) GRE T1-weighted images demonstrate smooth thickening of left adrenal gland (arrow), with signal intensity loss on out-of-phase sequence. Axial in-phase (c) and out-of-phase (d) GRE T1-weighted images show bilateral nodular thickening of adrenals in a patient with adrenal hyperplasia (arrows). Photomicrography HE 12.5x (e) and HE 50x (f) demonstrate nodules in the adrenal cortex, a typical finding of adrenal cortical hyperplasia (in patients with micronodular cortical hyperplasia). Differentiation between nodular hyperplasia and adenoma may be difficult at MRI.

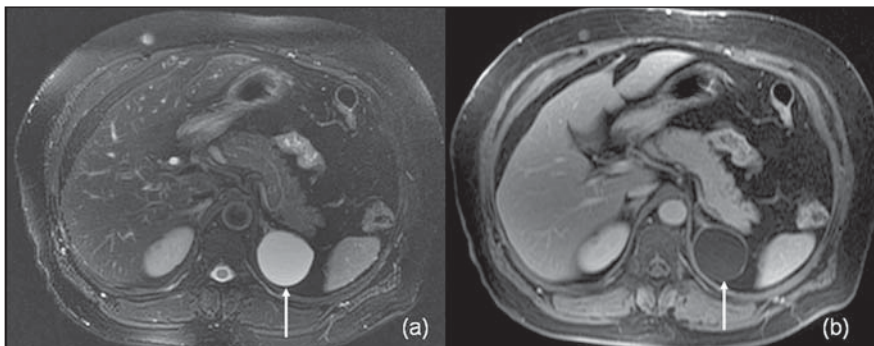


Figure 11. MRI axial FSE T2-weighted (a) and contrast-enhanced GRE T1-weighted images (b) of a simple cyst in left adrenal gland (arrow). In case of dubious T2-weighted images (simple cyst or lesion with hyperintense signal on T2-weighted sequences), like typical pheochromocytoma, the contrast agent may help in the differentiation, considering that in cysts there is no contrast uptake.

lymphangiectasic); 2) epithelial; 3) pseudocysts; 4) parasitic. Pseudocysts may be post-traumatic or postinfectious.

At MRI, a simple adrenal cyst is usually hypointense on T1-weighted images, and hyperintense on T2-weighted images (Figure 11). However, some of them may present with hemorrhagic content, with variable signal intensity depending on the stage of hemoglobin degradation. Cysts walls should be thin, without nodular components or contrast uptake. Besides, calcification may be present on the cyst wall

which can be better evaluated by CT. However, the utilization of long echo time and low flip angle GRE sequences may be of aid in the identification of calcium or hemosiderin artifacts.

Sometimes the differentiation between adrenal cysts/pseudocysts and pheochromocytomas is difficult, considering that both are hyperintense on T2-weighted sequences. In this situation, the utilization of a contrast agent is essential, considering the intense uptake by pheochromocytomas⁽³⁾.

Adrenal hemorrhage may be spontaneous (most rarely) or secondary to trauma. The majority of patients with adrenal hemorrhage do not present clinical signs of adrenal failure, and the diagnosis is incidentally achieved by means of imaging studies performed for other reasons. A traumatic adrenal hemorrhage may be idiopathic or usually secondary to stress, coagulation disorders, neonatal stress or tumors⁽²⁶⁻²⁸⁾.

Although CT is the imaging method of choice in the initial evaluation of adrenal hemorrhage, MRI not only can diagnose and evaluate hematomas, but also defines the moment of the event (that is to say its "age"). In the acute phase (during the first seven days) adrenal hemorrhage is seen as iso- or hypointense signal on T1-weighted sequences, and with remarkable hypointense signal on T2-weighted images (high concentration of intracellular deoxyhemoglobin). In the subacute phase (seven days to six to seven weeks after the event), adrenal hemorrhage is seen with hyperintense signal on T1- and T2-weighted sequences (paramagnetic effects of metemoglobin [Fe²⁺]) (Figure 12). In the chronic phase (after six to seven weeks) adrenal hemorrhage often appears with low signal

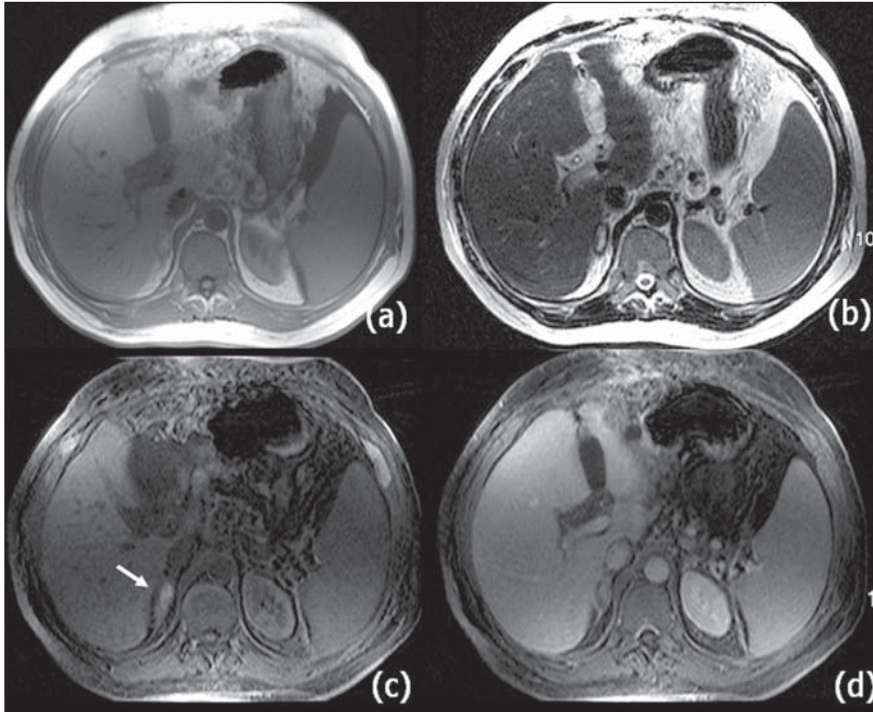


Figure 12. MRI axial slices. Axial in-phase (a) GRE T1-weighted image, axial FSE T2-weighted (b), axial GRE T1-weighted sequence with fat saturation before (c) and after (d) contrast injection in patient with right adrenal hemorrhage. Note the high signal on T1-weighted image representing methemoglobin (arrow).

intensity on T1- and T2-weighted images caused by hemosiderin deposition⁽²⁶⁾.

CONCLUSIONS

The increasing utilization of sectional imaging methods has improved the rates of incidental detection of adrenal lesions. Benign and malignant tumors are frequent and their characterization is of great clinical relevance. Besides identifying and characterizing adrenal tumors, MRI presents as an advantage over other methods: the possibility of differentiating adenomas from other tumors with higher sensitivity and specificity, mainly with the utilization of in-phase- and out-of-phase-GRE sequences. This is extremely important for oncologic patients. Its high-resolution, contrast between tissues, and multiplanar capacity allow accurate diagnosis, besides establishing the relationship between adrenal lesions and adjacent organs. Continuous technical innovation in MRI (higher magnetic fields, introduction of new coils, sequences and techniques) will result in an expansion of MRI applications in a near future.

Acknowledgement

Dr. Ruy Rodrigues Galves Jr., for his contribution with adrenal lymphoma images.

REFERENCES

1. Mayo-Smith WW, Boland GW, Noto RB, et al. State-of-the-Art. Adrenal imaging. *RadioGraphics*. 2001;21:995-1012.
2. Lockhart ME, Smith JK, Kenney PJ. Imaging of adrenal masses. *Eur J Radiol*. 2002;41:95-112.
3. Israel GM, Krinsky GA. MR imaging of the kidneys and adrenal glands. *Radiol Clin North Am*. 2003;41:145-59.
4. Mitchell DG, Crovello M, Matteucci T, et al. Benign adrenocortical masses: diagnosis with chemical shift MR imaging. *Radiology*. 1992;185:345-51.
5. Hussain HK, Korobkin M. MR imaging of the adrenal glands. *Magn Reson Imaging Clin N Am*. 2004;12:515-44.
6. Fishman EK, Deutch BM, Hartman DS, et al. Primary adrenocortical carcinoma: CT evaluation with clinical correlation. *AJR Am J Roentgenol*. 1987;148:531-5.
7. Krestin GP. Genitourinary MR: kidneys and adrenal glands. *Eur Radiol*. 1999;9:1705-14.
8. Namimoto T, Yamashita Y, Mitsuzaki K, et al. Adrenal masses: quantification of fat content with double-echo chemical shift in-phase and opposed-phase FLASH MR images for differentiation of adrenal adenomas. *Radiology*. 2001;218:642-6.
9. Bilbey JH, McLoughlin RF, Kurkjian PS, et al.

MR imaging of adrenal masses: value of chemical-shift imaging for distinguishing adenomas from other tumors. *AJR Am J Roentgenol*. 1995;164:637-42.

10. Mendonça BB, Lucon AM, Menezes CA, et al. Clinical, hormonal and pathological findings in a comparative study of adrenocortical neoplasms in childhood and adulthood. *J Urol*. 1995;154:2004-9.
11. Haider MA, Ghai S, Jhaveri K, et al. Chemical shift MR imaging of hyperattenuating (> 10 HU) adrenal masses: does it still have a role? *Radiology*. 2004;231:711-6.
12. Cirillo RL Jr, Bennett WF, Vitellas KM, et al. Pathology of the adrenal gland: imaging features. *AJR Am J Roentgenol*. 1998;170:429-35.
13. Kenney PJ, Wagner BJ, Rao P, et al. Myelolipoma: CT and pathologic features. *Radiology*. 1998;208:87-95.
14. Francis IR, Korobkin M. Pheochromocytoma. *Radiol Clin North Am*. 1996;34:1101-12.
15. Elsayes KM, Narra VR, Leyendecker JR, et al. MRI of adrenal and extraadrenal pheochromocytoma. *AJR Am J Roentgenol*. 2005;184:860-7.
16. Dunnick NR, Korobkin M. Imaging of adrenal incidentalomas: current status. *AJR Am J Roentgenol*. 2002;179:559-68.
17. Lucon AM, Pereira MAA, Mendonça BB, et al. Pheochromocytoma: study of 50 cases. *J Urol*. 1997;157:1208-12.
18. Blake MA, Kalra MK, Maher MM, et al. Pheochromocytoma: an imaging chameleon. *RadioGraphics*. 2004;24:S87-99.
19. Varghese JC, Hahn PF, Papanicolaou N, et al. MR differentiation of pheochromocytoma from other adrenal lesions based on qualitative analysis of T2 relaxation times. *Clin Radiol*. 1997;52:603-6.
20. Lonergan GJ, Schwab CM, Suarez ES, et al. Neuroblastoma, ganglioneuroblastoma, and ganglioneuroma: radiologic-pathologic correlation. *RadioGraphics*. 2002;22:911-34.
21. Falchook FS, Allard JC. CT of primary adrenal lymphoma. *J Comput Assist Tomogr*. 1991;15:1048-50.
22. Paling MR, Williamson BRJ. Adrenal involvement in non-Hodgkin lymphoma. *AJR Am J Roentgenol*. 1983;141:303-5.
23. Nacif MS, Jauregui GF, Mello RAF, et al. Linfoma adrenal primário bilateral com envolvimento do sistema nervoso central: relato de caso. *Radiol Bras*. 2005;38:235-8.
24. Doppman JL, Gill JR Jr, Miller DL, et al. Distinction between hyperaldosteronism due to bilateral hyperplasia and unilateral aldosteronoma: reliability of CT. *Radiology*. 1992;184:677-82.
25. Westra SJ, Zaninovic AC, Hall TR, et al. Imaging of the adrenal gland in children. *RadioGraphics*. 1994;14:1323-40.
26. Kawashima A, Sandler CM, Ernst RD, et al. Imaging of nontraumatic hemorrhage of the adrenal gland. *RadioGraphics*. 1999;19:949-63.
27. Hoeffel C, Legmann P, Luton JP, et al. Spontaneous unilateral adrenal hemorrhage: Computerized tomography and magnetic resonance imaging findings in 8 cases. *J Urol*. 1995;154:1647-51.
28. Araújo Neto SA, Rezende RT, Souza AS, et al. Hemorragia adrenal bilateral com trombose da veia renal direita e veia cava inferior em um recém-nascido. *Radiol Bras*. 2003;36:317-21.